Valence space techniques and QRPA vibrational mass parameters

Valence space techniques and QRPA vibrational mass parameters

I. Deloncle[1,2] and F. Lechaftois [2] and S. Péru [2]
[1]CSNSM, IN2P3/CNRS, 91405 Orsay Campus, FRANCE
[2]CEA, DAM, DIF 91680 Arpajon, FRANCE

E-mail: isabelle.deloncle@csnsm.in2p3.fr

Abstract. The vibrational mass parameters entering the quadrupolar 5DCH Hamiltonian are commonly obtained neglecting beyond mean-field correlations and the dynamical mean-field rearrangement. The Quasiparticle Random Phase Approximation (QRPA) framework would allow to avoid these disadvantages [1], if the computation time, when using density dependent force, was not prohibitive. Here, a significant time reduction is obtained by applying valence space (VS) techniques (energy cut-off and inert core) in QRPA calculations. The VS techniques allow to probe the physical content of the mass parameter. The QRPA mass parameter exhibit robustness toward VS limitations contrarily to the intrinsic QRPA outputs, that show deceptive appearance when an inert core is used. Excited states energy, and associated transition probabilities, should not be considered for optimizing the valence space limits.

1. Introduction

In the 5-Dimensional Collective Hamiltonian (5DCH) theory the Bohr Hamiltonian is built microscopically, without any free parameter. Starting from only one ingredient – a density-dependent force – the low-energy quadrupolar dynamics, involving five collective degrees of freedom, is obtained from self-consistent mean-field solutions. The reduction of the computation time, relatively to the GCM process, obtained thanks to the GOA approximation makes 5DCH a possible cornerstone for the construction of an "universal" approach describing, on the same foot and from only one nucleon-nucleon interaction, nuclei along the whole chart. Indeed, 5DCH calculations can be undertaken in light nuclei –as soon as the concept of mean-field is meaningful (for N, Z $\gtrsim$ 10)– as well as in the heaviest ones for which the computation time is manageable. It is worth recalling that this approach is not limited to axial symmetry, and implies a β,γ mapping. Yet, several drawbacks of 5DCH are known [1, 2], giving rise to a dependence of the result reliability on the nuclear deformation. Possible cure of 5DCH could be obtained by adding beyond mean-field correlations to the 5DCH vibrational mass parameters [1, 2, 3, 4]. In principle that could be achieved in Quasiparticle Random Phase Approximation (QRPA), but not in practice due to the prohibitive QRPA time consumption, in particular when using a density-dependent force. On another hand, the strong variations with the deformation of the vibrational mass parameters [5, 6] impose to compute them for a large amount of β,γ values. The time related cost is thus a key issue in the development of 5DCH cures, and our recent work [16], in that respect, represents an important breakthrough. Indeed, for the first time a vibrational mass parameter is obtained, in a reasonable computational time, within a HFB+QRPA approach built on a Gogny interaction (D1M). In our work, the computing time

reduction is reached by setting limitations on the valence space available for the quasi-particle (qp) excitations entering the QRPA calculations. The technique of the cut-off in the 2qp energy, that limits the upper single level involved in the excitation, has already been validated for phonon energy, with Skyrme [7] as well as with D1S [8]. Another way of limiting the valence space is used in standard shell model: the introduction of an inert core that put aside the lowest single-particle levels. We apply the cut-off technique and, for the first time, the inert core one, to the determination of mass parameters. Both the optimal 2qp energy cut-off value and the inert core size are determined according to the validity of the resulting mass parameters. With the same limitations the inaccuracy of calculated built-in QRPA outputs, namely phonon energies and reduced transition probabilities establish the robustness of mass parameters.

2. Formalism for vibrational mass parameters

2.1. From TDHFB to Inglis-Belyaev

In 5DCH calculations, the potential energy V, the three moments of inertia $\mathfrak{J}_i$ (with i$\in$ (x,y,z)) and the three vibrational mass parameters $B_{\mu\nu}$ (with$(\mu,\nu) \in (0,2)$) of the Bohr Hamiltonian

$$\mathcal{H} = V + \tfrac{1}{2}\sum_i \mathfrak{J}_i\omega_i^2 + \tfrac{1}{2}(B_{00}\dot{q_0}^2 + B_{22}\dot{q_2}^2 + B_{02}\dot{q_0}\dot{q_2}) \quad (1)$$

are determined microscopically at few tens of points of the sextant (β, $0° \leq \gamma \leq 60$ °) from statical constrained Hartree-Fock-Bogolyubov (CHFB) calculations. Usually the vibrational mass parameters are computed at the cranking order using the Inglis-Belyaev formula. This formula is established from time dependent Hartree-Fock (TDHFB) framework when assuming adiabaticity of the collective motion (ATDHFB) –that allows a perturbative development of the generalised density, stopped at the first (cranking) order– and neglecting the modification, time-odd, of the mean-field brought by the perturbated density. The dynamics is "restored" at the 5DCH diagonalisation stage. Indeed, in the Gaussian Overlap Approximation (GOA) of the Generalized Coordinate Method, the eigenstates of the 5DCH Hamiltonian are sought as superposition of CHFB states from different deformation. Different excited single-particle level configurations (or quasiparticle occupation (u,v)) are thus explored with deformation. At the deformation where a vibrational mass parameter B presents a peak, the $\hbar^2/2B$ term of the requantized 5DCH Hamiltonian is very small. In this way, configurations with high potential energy from that deformation can mix with configurations from near-CHFB minimum with similar requantized "mechanical" energy. Deformed low-energy 5DCH excited states can be obtained despite a spherical HFB minimum as in Tin isotopes [9, 4] or in ^{32}Mg [10] for example. The mass parameters being determinative for the dynamics, their computation should include as much physics as possible, such as dynamical mean-field rearrangement or beyond the mean-field correlations. The mean-field being a statical and particle independent (mostly uncorrelated) view of the nucleus, it can only partly include (in averaging) the correlations brought by the interaction. The Quasiparticle Random Phase Approximation (QRPA) formalism takes into account 2qp correlations excluded from HFB formalism (residual interaction). It is a possible path toward enriched vibrational mass parameter.

2.2. From TDHFB to QRPA

QRPA is another limit (small amplitude one) of TDHFB allowing to study the harmonic answer of a nucleus subjected, at its minimum of potential energy, to a small impulsion. The answer is sought as coherent (or correlated) superpositions of 2qp excitations, the phonons defined by:

$$\theta_n^+ = \sum_{kk'}(X^n_{kk'}\alpha_k^+\alpha_{k'}^+ - Y^n_{kk'}\alpha_k\alpha_{k'}), \quad (2)$$

$$\theta_n^+ \,|\,\mathrm{QRPA}\rangle = |\,\mathrm{n}\rangle \quad (3)$$

In the creation of a phonon, 2qp are deleted and 2qp are created together, with the X and Y amplitudes respectively, which are solutions of the equation:

$$\begin{pmatrix} A & B \\ B^* & A^* \end{pmatrix} \begin{pmatrix} X_n \\ Y_n \end{pmatrix} = \omega_n \begin{pmatrix} X_n \\ -Y_n \end{pmatrix} \tag{4}$$

In Equation 4 the matrix elements of A and B are calculated from the residual interaction. Nearly forty years ago, Vautherin [11] established the equivalence of the ATHFB mass parameter (related to the nuclear polarizability) and the cubic inverse energy weighted RPA sum rule :

$$B_{\mu\nu} = \frac{\hbar^2}{2} \frac{\mathcal{M}_{-3}(Q_{\mu\nu})}{\mathcal{M}_{-1}(Q_{\mu\nu})}, \quad \mu, \nu \in (0, 2) \tag{5}$$

The k^{th} order moment of the $Q_{\mu\nu}$ strength distribution is given by:

$$\mathcal{M}_{\rm k}(Q_{\mu\nu}) = \sum_n \omega^{\rm k} |\langle \phi \,|\theta_n^+ Q_{2\mu}|\, \phi\rangle\langle \phi \,|\theta_n^+ Q_{2\nu}|\, \phi\rangle| \tag{6}$$

Unfortunately, as already mentioned, the calculation time prevents the use of QRPA as it is for the 5DCH mass parameter. In the following, we restrict the number of 2qp excitations entering in Eq. (2) in order to evaluate Eq. (5).

3. Results

The study is performed on the $^{110-144}$Sn isotopes. A large variety of underlying single-particle level spectrum is then explored with N, as it would as a function of deformation in one nucleus. The $^{110-144}$Sn isotopes have their minimum of HFB energy at zero deformation, where the QRPA calculations will be performed. It allows to decorrelate the notion of valence space from deformation. Moreover, at zero deformation our study can be realized on B_{00} only, since the $B_{\mu\nu}$ fulfil the relation:

$$B_{00} = \frac{\hbar^2}{2} \frac{\mathcal{M}_{-3,00}}{[\mathcal{M}_{-1,00}]^2} = 2B_{20} = 4B_{22}. \tag{7}$$

The quasiparticles, inputs of the QRPA process, have been determined with the axial HFB code of ref.[12]. In HFB and in QRPA calculations, the effective interaction is D1M [13] and an harmonic oscillator basis with 11 major shells provides stabilized results in the $^{100-144}$Sn isotopes. The axial QRPA calculation have been achieved with the multi threads version [8] of the code detailed in [14]. The restriction on the quasiparticles is done by defining in the whole matrix QRPA sub-matrices, for which the diagonalization, fastest part of the QRPA process, is performed.

3.1. Mass parameter with 2qp energy cut-off

Here, the valence space is reduced by an energy cut-off set on the 2qp excitations (i.e the sum of the energies of the two qp involved in the excitation) keeping only 2qp excitations with energy below or equal that of the cut-off. One then assumes that high energy 2qp excitation play a minor role in the nuclear polarizability. A high enough cut-off value should provide a reasonable $B_{00_{\rm cut}}^{\rm no\ core}$, approximation of the value obtained without any valence space restriction, $B_{00_\emptyset}^{\rm no\ core}$, our absolute reference (full QRPA). (The symbol $\emptyset$ indicates calculations without any cut-off.)
In Figure 1 is drawn $R_{abs}(B_{00})=B_{00_{\rm cut}}^{\rm no\ core}/B_{00_\emptyset}^{\rm no\ core}$ as a function of A. The choice of a 2qp energy cut-off above 50 MeV is immediate. With cut-off energy below 50 MeV the $B_{00_{\rm cut}}^{\rm no\ core}$ values lie between 1.5 up to 13.5 times the $B_{00_\emptyset}^{\rm no\ core}$ one. It can be seen in the insert of the Figure 1,

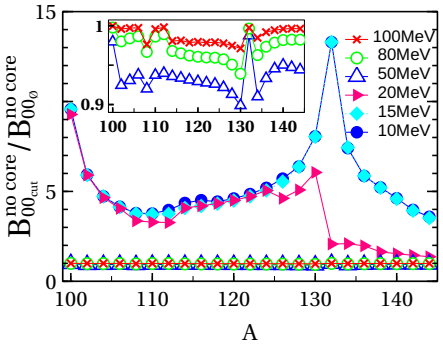

Figure 1. For different 2qp energy cut-off values and as a function of mass, ratio $R_{abs}(B_{00})$ (see text). A zoom on the ordinate around the value of 1.0 is shown in the insert.

that better than 90% in mean of the reference value (with the exceptio of ^{130}Sn) is reached with energy cut-offs from 50-MeV. It would be interesting to get more information in the intermediate 20 - 50 MeV energy range, by setting for example a 40 MeV cut-off. This is in progress.
Figure 1 presents effects due to the underlying single-particle level density. The curves obtained with small energy cut-offs present typical shell effects, large peaks at shell closures. Between A=100 and A=132, 2qp benefit by the shells lying between the gaps, to generate excitations with little energy. This leads to the parabolic shape, with a minimum around N=62 ($\nu g_{7/2}$ occupancy) of the 10, 15 and 20 MeV curves. They are superimposed, thus 2qp excitations with at most 10 MeV give the main low energy contribution for A=100-132. However, from A=126, 2qp excitations of 15-20 MeV increase. Better values are obtained in $^{126-130}$Sn with a 20 MeV cut-off. In $^{132-144}$Sn (from N $\geq$82), after a stiff drop (A=130-132, not observed at A=100-102), the 2qp excitations of 15-20 MeV energy become essential, leading to a mass parameter twice the reference only. The previous features indicate that 2qp excitations with "low" energy carry fine structure information, they can not be neglected. The use of a high- and low-cut filter for computing vibrational mass parameter is thus excluded.
It is worth noting that with Tamm-Dancoff approximation, we obtained $B_{00_{\text{TDA}}}$ greater than $B^{\text{no core}}_{00_\emptyset}$ in all Sn isotopes[16]. Their ratio (1.3 in mean) presents also variations as a function of A, but a minimum at N=82. Neglecting 2qp excitations with energy higher than 20 MeV, or ground-state correlations results in overestimating B_{00}. Inversely here, from 50 MeV cut-off, the obtained mass parameters are satisfactory underestimate (better than 90%) of the expected value (see insert of Fig 1). A fine agreement is obtained at shell closures, structure effects are still visible. In our previous work $B^{Inglis\text{-}Belyaev}_{00}$ commonly used in 5DCH, was found to underestimate 1.3 times, in mean, $B^{\text{no core}}_{00_\emptyset}$, with a larger discrepancy at shell closure.
The valuable results obtained with a 50-MeV energy cut-off validates the hypothesis of the high energy 2qp excitations playing only a minor role in the mass parameter value. Moreover, a 50-MeV energy cut-off provides a reduction in computation time of a factor 16.

3.2. Mass parameter with inert core and 2qp energy cut-off

Never applied in QRPA, but largely and commonly used in standard shell model calculation, is the technique consisting in freezing deep qp lying at the bottom of the mean-field, in an inert (non excitable) core. We directly imported this technique in our QRPA calculations and build submatrices by selecting qp that are rows and columns of the whole QRPA matrices.
We performed the calculations with five different cores, ^{40}Ca, ^{48}Ca, ^{56}Ni, ^{70}Ca, and ^{78}Ni. The results obtained with the two first cores are sufficient to draw conclusions. On Figure 2 are reported $R_{abs}(B_{00})$, ratios of $B^{^{40}\text{Ca}}_{00_{\text{cut}}}$ (a)) or $B^{^{48}\text{Ca}}_{00_{\text{cut}}}$ (b)) over $B^{\text{no core}}_{00_\emptyset}$, for $^{100-144}$Sn and as a function of 2qp energy cut-off. A common feature appears at a first glance in the results drawn in Figure 2a) and b): the dramatic change in the slope and values of the curves when the energy cut-off reaches 50 MeV. Below, the mass parameter are overestimated, the slopes

exhibit important variations according to the neutron number. Above, only slight variations as a function of N are observed (see inserts). However, in the left panel insert, the curves merge toward each other when converging to relevant no cut-off values – lying within 90 percent of the $B^{\text{no core}}_{00_\emptyset}$–. In the right panel the "inter convergence" of the curves toward each other is less pronounced, and their asymptotic values are less satisfactory, ranging between 1.05 and 1.25. For the heavier inert cores (not shown here), the curves diverge between themselves. Such effect may be of great interest to check the pertinence of the convergence process. In Table 1, are

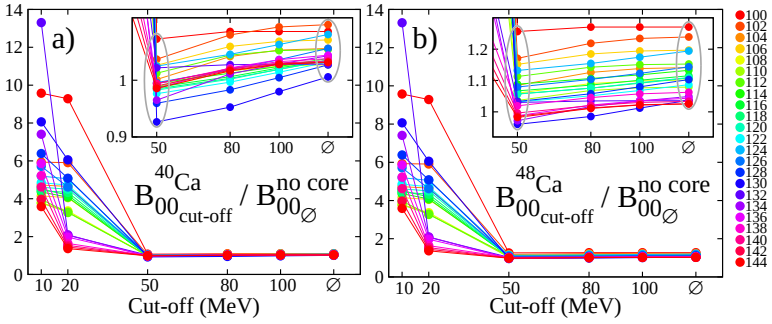

Figure 2. As a function of the cut-off value, ratios $R_{abs}(B_{00})$ (see text) in $^{100-140}$Sn isotopes with a) ^{40}Ca (left) or b) ^{48}Ca as inert core. In the insert, ellipses allow to highlight the convergence of the curves toward themselves.

reported the mean value and the standard deviation of the distribution of the asymptotic values of the ratio $R_{abs}(B_{00})=B^{\text{core}}_{00_\emptyset}/\ B^{\text{no core}}_{00_\emptyset}$ obtained for different cores without energy cut-off. All the

Table 1. Mean value and standard deviation of the distribution over the $^{100-140}$Sn isotopes of the asymptotic values of $R_{abs}(B_{00})$ according to different inert cores.

	^{40}Ca	^{48}Ca	^{56}Ni	^{70}Ca	^{78}Ni
mean val.	1.04	1.11	1.24	1.53	1.70
stdev	0.02	0.07	0.09	0.29	0.34

asymptotic values are, from ^{56}Ni, large overestimations (by a factor at least 1.15) of the mass parameter. In this paper, overestimation was previously mentioned when neglecting ground-state correlations or 2qp excitations of less than 50 MeV. Here, of course, it is due to the inert core insertion, which reduces *de facto* ground-state correlations, since many qp do participate anymore to Eqs (2) and (4). Frozen in "large" inert core (N, Z $\geq$ 28), there are qp, not so deep, that would have participated to in-shells excitations with little energy. Indeed, their excitation toward shells above the Fermi level would have required very high energy.

With a ^{48}Ca inert core, few Sn isotopes have a mass parameter slightly underestimated when using a 50-MeV energy cut-off, see Figure 2. They also have asymptotic values lying very near the reference. For these isotopes it should be possible to take benefit of the ^{48}Ca inert core to reduce more drastically the computation time. Of course, for systematic calculations, the results summed up in Table 1 and Figure 2 rule out the use of any core heavier than ^{40}Ca in combination with a 50-MeV cut-off. Fortunately, the computation time is significantly reduced, by a factor 2, when using this inert core. Using both a 50-MeV energy cut-off and the ^{40}Ca inert core the total gain in computation time reaches up to a factor 30. If results using these two limitations are robust, it should give room enough for facing calculations of QRPA mass parameters, with a valence space, in most of the nuclei at any deformation. In order to check the robustness of our mass parameter, and to assess our hypothesis, calculations of intrinsic QRPA outputs, i.e. phonon energy and their reduced transition probability with valence space have been undertaken.

3.3. QRPA outputs with 2qp energy cut-off

In Figure 3 are drawn as a function of the 2qp energy cut-off, the variation of the 2_1^+ and 3_1^- energies, and of their associated reduced transition probability, relatively to the reference values obtained without cut-off (and no core). Opposite trends are observed for the excited state energies and the transition probabilities. At 50 MeV, neither the energies nor the

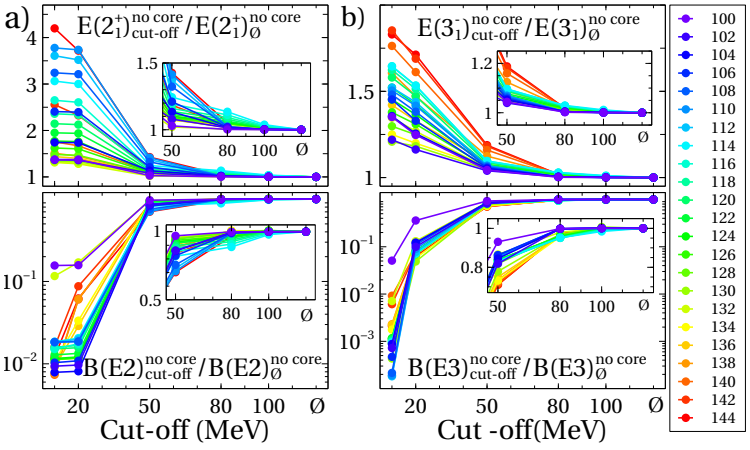

Figure 3. As a function of the cut-off value, ratio $R_{abs}(E(2_1^+))$ (a)) and $R_{abs}(E(3_1^-))$ (b)) (see text). The color to mass correspondence is given in the palette at the right. A zoom on the ordinate is shown in the insert.

transition probabilities are converged. The convergence is only obtained from 100 MeV (80 MeV respectively) cut-off for the 2_1^+ (3_1^- resp.) energy and transition probability. The 2qp excitations with energy lower or equal to 50 MeV, that make 90% of the vibrational mass parameter B_{00}, represent of the order of 70% only of what is needed to build the first excited states. The lack of high-energy 2qp excitations has heavy consequences. Inversely, it confirms their secondary role in the polarizability. In Figure 3, one can also notice, on the one hand, the greater sensitivity of the transition probability, as compared to the excited state energy, to missing 2qp excitations with energy comprised between 20 and 50 MeV, and on the other hand, the substantial improvement brought by 2qp excitation of energy between 10 and 20 MeV in $E(3_1^-)$) and B(E3) only.

3.4. QRPA outputs with inert core

In Table 2, are reported the mean value and the standard deviation of the asymptotic values (i.e without energy cut-off) of the ratios $R_{abs}(X)=X_{\emptyset}^{core}/\ X_{\emptyset}^{no\ core}$, where X stands for $E(2_1^+)$ or $E(3_1^-)$, obtained with different cores. Once more the results for the 2_1^+ differ from those for the 3_1^-. The latter leads to better convergence properties, though not sufficients to give valuable results with any of the cores used here. It is worth noting that we obtained satisfactory values for both state energies when using a much smaller inert core, ^{16}O.

Table 2. Mean value and standard deviation of the distribution over the $^{100-144}$Sn isotopes of the asymptotic values of (a)) $R_{abs}(E(2_1^+))$ and (b)) $R_{abs}(E(3_1^-))$ for different inert cores.

		^{40}Ca	^{48}Ca	^{56}Ni	^{70}Ca	^{78}Ni
$E(2_1^+)$	mean val.	1.39	1.47	1.65	1.70	1.79
	stdev	0.31	0.36	0.49	0.54	0.61
$E(3_1^-)$	mean val.	1.16	1.19	1.27	1.30	1.34
	stdev	0.06	0.07	0.10	0.11	0.13

As a last result is shown in Figure 4 the remarkable deceptive convergence scheme of the relative ratio $R_{rel}(E(2_1^+))=E(2_1^+)^{core}_{cut-off}/\ E(2_1^+)^{core}_{\emptyset}$ obtained with ^{78}Ni as inert core. The convergence toward the asymptotic no cut-off value obtained with a given core has the appearance of a fast and efficient process, despite large differences obtained between the asymptotic no cut-off value with a core and the absolute value (no cut-off, no core). These results are astonishing since

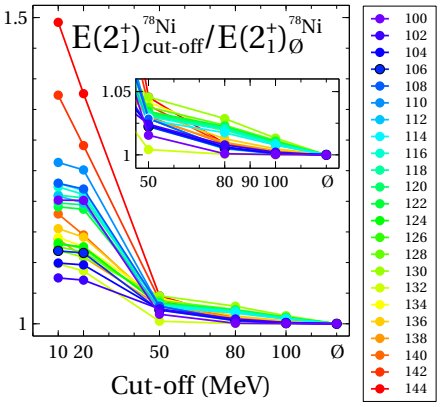

Figure 4. As a function of the cut-off value, ratios $R_{rel}(E(2_1^+))$ (see text) in $^{100-140}$Sn isotopes for the ^{78}Ni inert core. The color to mass correspondence is given by the palette at the right. A zoom on ordinate is provided in the insert.

in standard shell models calculations larger cores are commonly used. It would be possible to perform the required normalizations (on each multipolarity) using some absolute values – get full QRPA calculations for few points being feasible –. That would be, however, counter productive since time-consuming. Moreover it would lead to the loss of the "universal" and coherent character of the 5DCH approach, which consists in using one density-dependent force only to describe nuclei over the whole chart.

4. Conclusions

The introduction of the valence space notion in QRPA calculations, via 2qp energy cut-off and inert core, is an important breakthrough for the 5DCH framework. It offers a glimpse of a possible path toward valuable vibrational mass parameter calculations on the required few tens of (β,γ) points. The vibrational mass parameters appear very robust against valence space limitations, allowing a factor of 30 to be reached in the computation time reduction. On the contrary, unreliable values are obtained for intrinsic QRPA outputs in the same approximations, that exhibit deceptive convergence.

[1] J.-P. Delaroche, M. Girod, J. Libert, H. Goutte, S. Hilaire, S. Péru, N. Pillet and G.F. Bertsch, Phys. Rev. C **81**, 014303 (2010).
[2] G.F. Bertsch, M. Girod, S. Hilaire, J.-P. Delaroche, H. Goutte and S. Péru, Phys. Rev. Lett. **99**, 032502 (2007).
[3] M. Bender and P.-H. Heenen, Phys. Rev. C **78**, 024309 (2008).
[4] S. Péru and M. Martini, Eur. Phys. J. A **50**, 88 (2014).
[5] B. Mohammed-Azizi, Electronic J. Theor. Phys. **9**, No. **27** (2012) 143-158.
[6] E.Kh. Yuldashbaeva, J. Libert, P. Quentin and M. Girod, Phys. Lett. B **461**, 1 (1999).
[7] K. Yoshida and N. Van Giai, Phys. Rev. C **78**, 064316 (2008).
[8] S. Péru, G. Gosselin, M. Martini, M. Dupuis, S. Hilaire and J.-C. Devaux, Phys. Rev. C **83**, 014314 (2011).
[9] J. Libert, B. Roussière and J. Sauvage, Nucl. Phys. A 786, 47 (2007)
[10] S. Péru, M. Girod and J.-F. Berger, E. P. J. A **9**, 35 (2000)
[11] D. Vautherin, Phys. Lett. Vol. 69B Numb. 4, 393 (1977)
[12] S. Hilaire and M. Girod, Eur. Phys. J. A **33**, 237 (2007).
[13] S. Goriely, S. Hilaire, M. Girod and S. Péru, Phys. Rev. Lett. **102**, 242501 (2009).
[14] S. Péru and H. Goutte, Phys. Rev. C **77**, 044313 (2008).
[15] J. Libert, M. Girod and J.-P. Delaroche, Phys. Rev. C **60**, 054301 (1999).
[16] F. Lechaftois, I. Deloncle and S. Péru, Phys. Rev. C **92**, 034315 (2015).